Food Control 75 (2017) 246–254

Contents lists available at ScienceDirect

Food Control

journal homepage: www.elsevier.com/locate/foodcont

Subsurface inspection of food safety and quality using line-scan spatially offset Raman spectroscopy technique

Jianwei Qin [a], Moon S. Kim [a, *], Kuanglin Chao [a], Walter F. Schmidt [a], Sagar Dhakal [a], Byoung-Kwan Cho [b], Yankun Peng [c], Min Huang [d]

[a] USDA/ARS Environmental Microbial and Food Safety Laboratory, Beltsville Agricultural Research Center, 10300 Baltimore Ave., Beltsville, MD 20705, USA
[b] Department of Biosystems Machinery Engineering, College of Agricultural and Life Science, Chungnam National University, 99 Daehak-ro, Yuseoung-gu, Daejeon 305-764, South Korea
[c] College of Engineering, China Agricultural University, 17 Qinghua East Road, Haidian, Beijing 100083, China
[d] Key Laboratory of Advanced Process Control for Light Industry (Ministry of Education), Jiangnan University, 1800 Lihu Ave., Wuxi, Jiangsu 214122, China

ARTICLE INFO

Article history:
Received 30 September 2016
Received in revised form
6 December 2016
Accepted 7 December 2016
Available online 8 December 2016

Keywords:
Raman spectroscopy
Lasers
Subsurface detection
Food quality
Food safety
Mixture analysis

ABSTRACT

Subsurface inspection of food and agricultural products is challenging for optical-based sensing techniques due to complex interactions between light and heterogeneous or layered samples. In this study, a method for subsurface food inspection was presented based on a newly developed line-scan spatially offset Raman spectroscopy (SORS) technique. A 785 nm point laser was used as a Raman excitation source. The line-shape SORS data from the sample was collected in a wavenumber range of 0–2815 cm^{-1} using a detection module consisting of an imaging spectrograph and a CCD camera. Two layered samples, one by placing a 1 mm thick plastic sheet cut from original container on top of cane sugar and the other by placing a 5 mm thick carrot slice on top of melamine powder, were created to test the subsurface food inspection method. For each sample, a whole set of SORS data was acquired using one CCD exposure in an offset range of 0–36 mm (two sides of the incident laser point) with a spatial interval of 0.07 mm. Raman spectra from the cane sugar under the plastic sheet and the melamine powder under the carrot slice were successfully resolved using self-modeling mixture analysis (SMA) algorithms, demonstrating the potential of the technique for authenticating foods and ingredients through packaging and evaluating internal food safety and quality attributes. The line-scan SORS measurement technique provides a rapid and nondestructive method for subsurface inspection of food safety and quality.

Published by Elsevier Ltd.

1. Introduction

Safety and quality examination is an important step in food production process, as many factors, such as stricter rules from regulatory agencies, customers' demands for safer and higher quality foods, and increasing foodborne illness outbreaks, have been continuously putting challenges on food inspection technologies. A variety of optical sensing techniques (e.g., ultraviolet, visible, fluorescence, Raman, infrared, and terahertz) have been researched for food safety and quality applications, in which the majority has focused on inspecting food surfaces using spectroscopy and imaging techniques. Subsurface inspection of food and agricultural products, such as detection of food adulterants through packaging and evaluation of flesh quality under fruit skin, is a challenging task for optical-based techniques due to complex interactions between light and heterogeneous or layered samples. Advanced sensing techniques that are routinely used in the medical field, such as ultrasound (Awad, Moharram, Shaltout, Asker, & Youssef, 2012), x-ray (Mathanker, Weckler, & Bowser, 2013), and magnetic resonance imaging (MRI) (Schmidt, Sun, & Litchfield, 1996), have been adopted to evaluate internal attributes of the food, such as detecting foreign objects and defects in food materials and estimating internal physical structure of the food. However, these techniques generally cannot be used for food composition analysis due to lack of compound-specific spectral information.

Spatially resolved spectroscopy techniques have been investigated for obtaining subsurface composition information. The basic principle is to separate a point light source and a detector to allow light to travel through deep area of a sample so that subsurface

* Corresponding author. USDA/ARS/EMFSL, Bldg. 303, BARC-East, 10300 Baltimore Ave., Beltsville, MD 20705-2350, USA.
E-mail address: moon.kim@ars.usda.gov (M.S. Kim).

http://dx.doi.org/10.1016/j.foodcont.2016.12.012
0956-7135/Published by Elsevier Ltd.

signals can be retrieved from the light coming out of the sample surface. The concept has been adopted by reflectance and fluorescence measurement techniques, such as spatially resolved diffuse reflectance (Dam et al., 2001), fluorescence (Hyde, Farrell, Patterson, & Wilson, 2001), hyperspectral reflectance imaging (Qin & Lu, 2008), and visible/near-infrared spectroscopy (Xiong, Li, & Lin, 2012). Since visible, near-infrared, and fluorescence spectra are typically characterized by broad peaks, the mixed spectra from different sample layers are generally difficult to be mathematically resolved and assigned to the individual components. Also, light penetration depth in the reflectance and fluorescence measurements is usually limited by the relatively low intensity of the light sources (e.g., halogen and LED lights).

Raman spectroscopy is a technique capable of analyzing composition of a target with high specificity using narrow and sharp peaks typically shown in a spectrum, and it is able to obtain surface and subsurface sample information using powerful narrowband lasers as excitation sources. Three major Raman measurement modes are illustrated in Fig. 1. Backscattering geometry (Fig. 1a) is the most widely used mode owing to its simplicity and convenience. In a typical setup, a laser and a detector are arranged on the same side of the sample. The detector acquires backscattered Raman signals from the laser incident point. The backscattering Raman signals have a strong contribution from the surface layer of the sample, which generally cannot be used to retrieve internal information from heterogeneous or layered samples. In transmission geometry (Fig. 1b), the laser and the detector are arranged on the different sides of the sample. The detector acquires forward-scattered Raman signals that pass through the sample. The practical use of the transmission Raman spectroscopy was improved during its development for pharmaceutical applications (Matousek & Parker, 2006). The technique greatly suppresses the Raman and fluorescence signals originated from the sample surfaces (e.g., tablet coatings and capsule shells), making it suitable for bulk composition analysis of diffusing and translucent materials, such as composition analysis of single soybeans (Schulmerich et al., 2012) and corn kernels (Shin, Chung, & Kwak, 2012), and differentiation of geographical origins of rice (Hwang, Kang, Lee, & Chung, 2012). However, the transmission method cannot resolve the spectra from individual layers of the sample.

Spatially offset Raman spectroscopy (SORS) (Fig. 1c) is a technique that intends to retrieve layered subsurface information by collecting Raman scattering signals from a series of surface positions laterally offset from the excitation laser (Matousek et al., 2005). The offset spectra exhibit different sensitivities to the Raman signals from the surface and the subsurface layers. The contribution of the Raman signals from the deep layers gradually outweighs that from the top layer as the source-detector distance increases. Spectral mixture analysis algorithms can be applied to an array of the SORS data to extract pure Raman spectra of the individual layers. Hence physical/chemical/biological information of the subsurface layers can be obtained based on the comparisons between the decomposed spectra and the reference Raman spectra. The SORS technique was initially developed for biomedical and pharmaceutical applications, such as noninvasive evaluation of human bone *in vivo* (Matousek et al., 2006) and authentication of pharmaceutical products through packaging (Eliasson & Matousek, 2007). Recently the technique has been used for evaluating food and agricultural products, such as nondestructive evaluation of internal maturity of tomatoes (Qin, Chao, & Kim, 2012) and quality analysis of salmon through the skin (Afseth, Bloomfield, Wold, & Matousek, 2014).

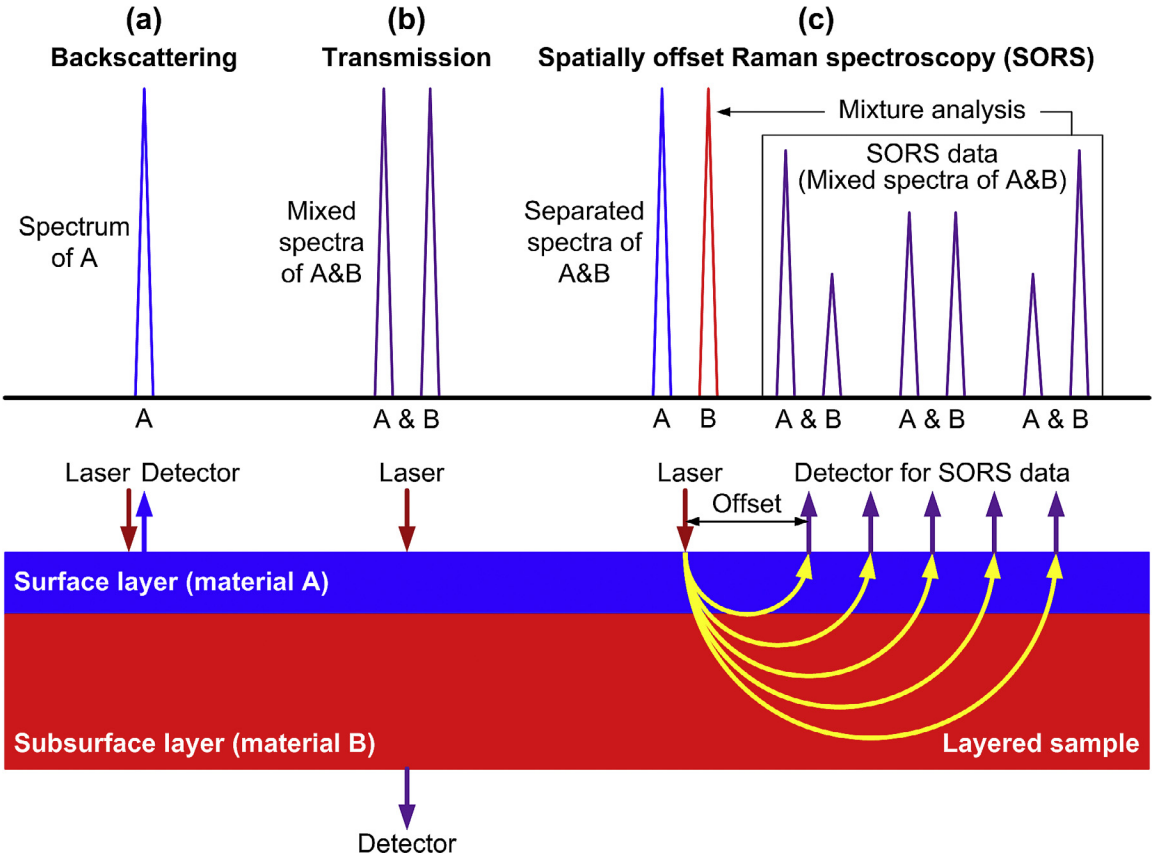

Fig. 1. Raman measurement modes: (a) backscattering, (b) transmission, and (c) spatially offset Raman spectroscopy.

Optical fiber probes, such as single fiber probe with mechanical movement (Afseth et al., 2014; Matousek et al., 2005; Qin et al., 2012) and fiber probe array with patterned excitation and collection (e.g., annular fiber probe and fiber bundle) (Keller et al., 2011; Matousek et al., 2006; Wang, Ding, Lu, & Bi, 2014), are commonly used in applying the SORS technique for different applications. The fiber probe methods are either slow (single fiber probe) or restricted in offset range and interval selection (fiber probe array) for collecting the spatially offset Raman spectra. We recently developed a new method to perform the SORS measurement using a line-scan Raman imaging system (Qin et al., 2016). The line-scan SORS technique realized simultaneous acquisition of a series of Raman spectra in a broad offset range with a narrow spatial interval using a single scan (i.e., one CCD exposure). The technique is more flexible and efficient than the methods using the fiber probes in implementing the SORS technique, and it has great potential for rapid and nondestructive subsurface inspection of food and agricultural products. This study aimed to demonstrate example applications of the line-scan SORS technique for subsurface evaluation of food safety and quality. Specific objectives were to:

- Use a line-scan Raman measurement system to acquire spatially offset Raman spectra from the samples;
- Create layered samples to test the line-scan SORS technique for detection of subsurface Raman-active analytes; and
- Develop spectral analysis algorithms for the SORS data to extract pure Raman signatures from surface and subsurface layers.

2. Materials and methods

2.1. Line-scan spatially offset Raman spectroscopy system

A Raman spectroscopy system (Fig. 2), which was assembled based on a line-scan Raman imaging system originally developed for high-throughput macro-scale chemical imaging for rapid food safety and quality inspection (Qin, Chao, Cho, Peng, & Kim, 2014), was used to collect spatially offset Raman spectra from the samples. The system utilized a 785 nm point laser (I0785MM0500MF, Innovative Photonic Solutions, Monmouth Junction, NJ, USA) as a Raman excitation source for the SORS measurement. The laser light was delivered and focused on the sample surface via an optical fiber and a laser focus unit, which consisted of a fiber optic collimator, a 785 nm laser-line bandpass filter, and a 50 mm focus lens. The incident angle of the laser was around 30° as the focus unit was arranged obliquely. On the sample surface, the laser point was approximately 1.0 mm in diameter with a power of 350 mW. A detection module consisting of a Raman imaging spectrograph (ImSpector R10E, Specim, Oulu, Finland) and a 16-bit CCD camera (iKon-M 934, Andor Technology, South Windsor, CT, USA) was used to acquire the spatially offset Raman scattering signals from the samples. The imaging spectrograph received light from a scanning line across the laser incident point via a 30 μm wide input slit. After passing through a prism-grating-prism (PGP) component of the spectrograph, the acquired light was dispersed into different wavelengths and then projected onto the CCD to create a 2-D image (1024 × 1024 pixels) with both spatial and spectral information.

The CCD, with quantum efficiency greater than 90% at 800 nm and about 45% at 1000 nm, was thermoelectrically cooled to −65 °C to minimize the dark current during spectral data acquisition. A C-mount lens with 35 mm focal length (Xenoplan, Schneider Optics, Van Nuys, CA, USA) was attached to the spectrograph for aperture and focus adjustment. The light signals at and below the laser wavelength of 785 nm (i.e., Rayleigh and anti-Stokes scattering) were blocked by two identical long-pass filters (Semrock, Rochester, NY, USA), which were placed in the connection area of the spectrograph and the lens. The Raman system was housed within an aluminum-framed enclosure with black foam boards to avoid the influence of ambient light. The system was found to cover a Raman shift range from −745 to 2815 cm^{-1} with a full width at half maximum (FWHM) spectral resolution of 14 cm^{-1}. In-house software was developed using LabVIEW with Vision Development Module (National Instruments, Austin, TX, USA) to fulfill parameterization and data-transfer functions. Details of the system description can be found in our previous methodology papers (Qin et al., 2014, 2016).

2.2. Experimental samples and procedures

Two types of layered samples were created to test the capability of the line-scan SORS technique for subsurface inspection of food samples. The first layered sample was prepared to test the potential of authenticating foods and ingredients through packaging. Cane sugar packed in a yellow plastic container (Domino Foods, Baltimore, MD, USA) was used for this demonstration purpose (Fig. 3a). The cane sugar was filled up in a custom-designed nickel container (low Raman and fluorescence signals) with a sample holding volume of 50 mm × 50 mm × 10 mm (Fig. 3b). A piece of plastic sheet (1 mm thick) cut from the original container was put on top of the container to completely cover the sugar sample for the SORS measurement (Fig. 3c). The second layered sample was prepared to test the potential of evaluating internal safety and quality attributes of the food. A fresh orange carrot from a local supermarket was sliced to a thickness of 5 mm along the cross section using a food slicer with adjustable thickness control (GS300, General Slicing, Weston, FL, USA). The carrot slice was placed on top of melamine powder (Sigma-Aldrich, St. Louis, MO, USA) to create a two-layer sample. The top layer of the carrot slice represented a general vegetable with Raman scattering features. The bottom layer of the melamine powder was chosen to symbolize a subsurface Raman-active analyte in food safety and quality evaluation. The carrot-on-melamine sample was placed in a Petri dish (Fisher Scientific, Pittsburgh, PA, USA) with a diameter of 47 mm.

For the two layered samples, efforts were made to flatten the surfaces of the top layers and the bottom layers to avoid gaps between them. A height adjustable stage was used to position the samples for the SORS measurement so that a lens-to-sample distance was approximately 20 cm. The length of the instantaneous field of view (IFOV) of the Raman system was determined as 72 mm at this working distance. The maximum spatial resolution along the scanning line direction can be estimated as 72 mm/1024 pixels = 0.07 mm/pixel. The laser incident point on the sample surface was positioned on the center of the 72 mm scanning line. Hence under this setup, spatially offset Raman spectra can be collected in an offset range of 0–36 mm (two sides of the incident laser point) with a spatial interval of 0.07 mm (no CCD binning along the spatial dimension). The samples were line scanned by the Raman system using a CCD exposure time of 10 s, resulting in a 1024 × 1024 spatial-spectral scattering image for each sample. A dark current image was collected with the laser off and a cap covering the lens, and it was subtracted from the original sample images. Only the subtracted images were used for further analysis. In addition to the layered samples, the SORS measurements using the same setup were also conducted to the individual pure samples (i.e., plastic sheet, cane sugar, carrot, and melamine) to provide reference spectra and also for the purpose of comparison.

2.3. Raman spectral analysis

Self-modeling mixture analysis (SMA) was used to analyze the

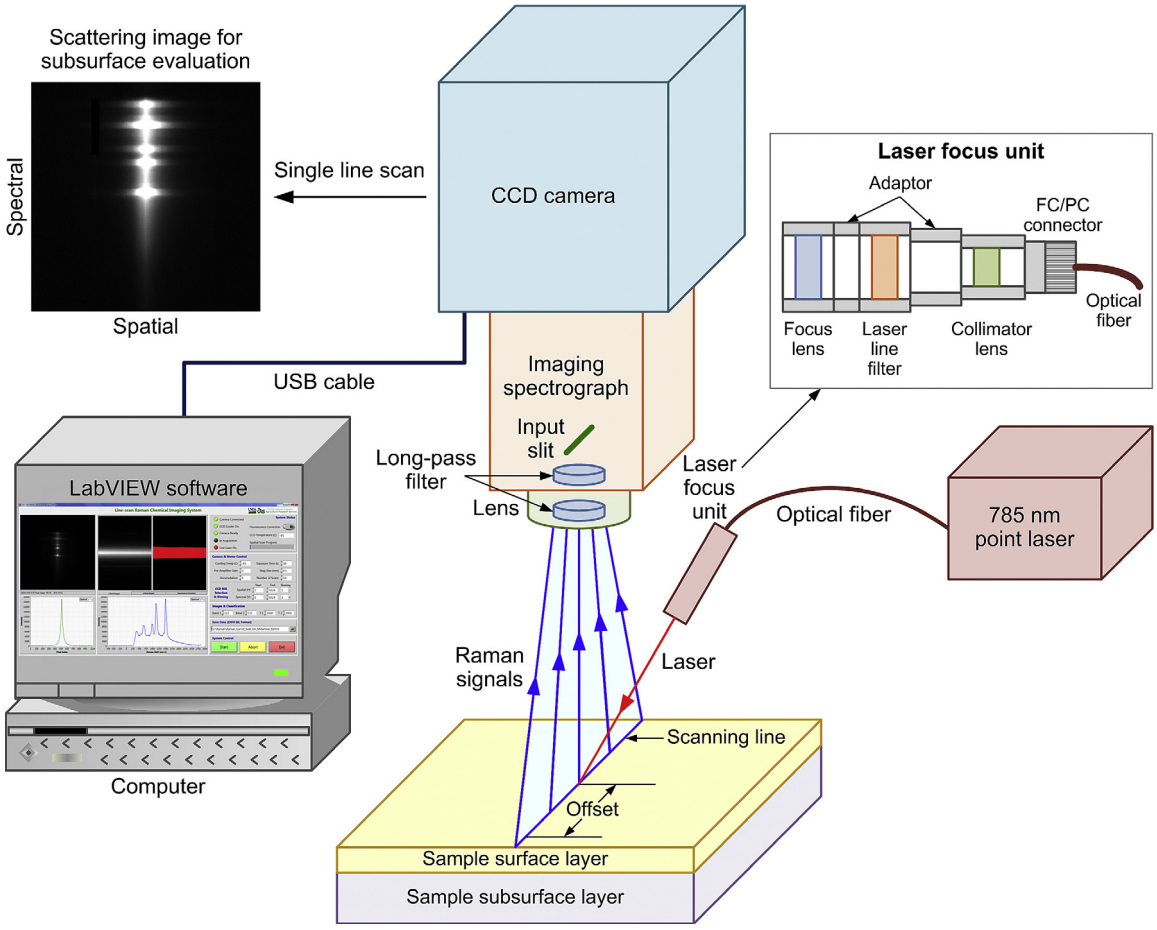

Fig. 2. Line-scan spatially offset Raman spectroscopy system for subsurface evaluation of layered samples.

spatially offset Raman spectra from the layered samples to extract Raman signatures of the surface and the subsurface layers. SMA is a powerful spectral analysis technique that can resolve a mixture of compounds without knowing the prior spectral information of the individual components (Windig & Guilment, 1991). A spectral data matrix can be decomposed into outer product of pure component spectra (or factors) and contributions (or scores) by the SMA method. The extracted pure component spectra can be used to identify the compositions of a mixture. In this study, a function named *Purity* provided by PLS_Toolbox (Eigenvector Research, Wenatchee, WA, USA) was used to conduct SMA for each set of the spatially offset Raman spectra. Performing SMA requires the expected number of the pure components to be predefined. For a mixture consisting of an unknown number of compositions, an overestimated component number is usually used for the calculation (Windig & Guilment, 1991). The resolved spectra are then examined to determine the appropriate number of the pure components. The compositions of the layered samples tested in this study (i.e., plastic sheet and cane sugar, and carrot and melamine) were known. The number of the pure components was selected as four for both sets of the SORS data. The spatial ranges of the SORS data used in SMA were determined by examining the spatial profiles extracted at different wavenumbers from the 2-D Raman spatial-spectral images. The spectral data analysis procedures described above were executed using in-house computer programs developed by MATLAB (MathWorks, Natick, MA, USA).

3. Results and discussion

3.1. SORS measurement results for plastic sheet and cane sugar samples

The SORS measurement results for the plastic sheet and cane sugar samples are summarized in Fig. 4. Fig. 4b shows reference Raman spectra of plastic sheet and cane sugar in the wavenumber range of 0–2815 cm^{-1}. The two original spectra share a similar fluorescence baseline with intensities gradually decreasing from short to long wavenumbers. The Raman spectrum of the plastic sheet is featured with four peaks in a narrow spectral region from 1000 to 1500 cm^{-1}. Another peak was also observed around 2778 cm^{-1}. The Raman features of the cane sugar are a series of adjacent peaks in the wavenumber range of 300–1500 cm^{-1}. The highest Raman peaks of the plastic sheet and the cane sugar appeared at 1438 and 531 cm^{-1}, respectively. The 1438 cm^{-1} and the 531 cm^{-1} vibrational modes can be assigned to CH_3 asymmetrical bending of polypropylene plastic (Arruebarrena de Báez, Hendra, & Judkins, 1995) and to deformation at site C5 of the fructofuranosyl ring of cane sugar (Brizuela et al., 2012), respectively. Meanwhile, the Raman intensities of both cane sugar at 1438 cm^{-1} and plastic sheet at 531 cm^{-1} are relatively low. Thus the 1438 cm^{-1} peak of the plastic sheet and the 531 cm^{-1} peak of the cane sugar were chosen as major Raman features for identification and differentiation of the two materials in the scattering images and the spatially offset Raman spectra.

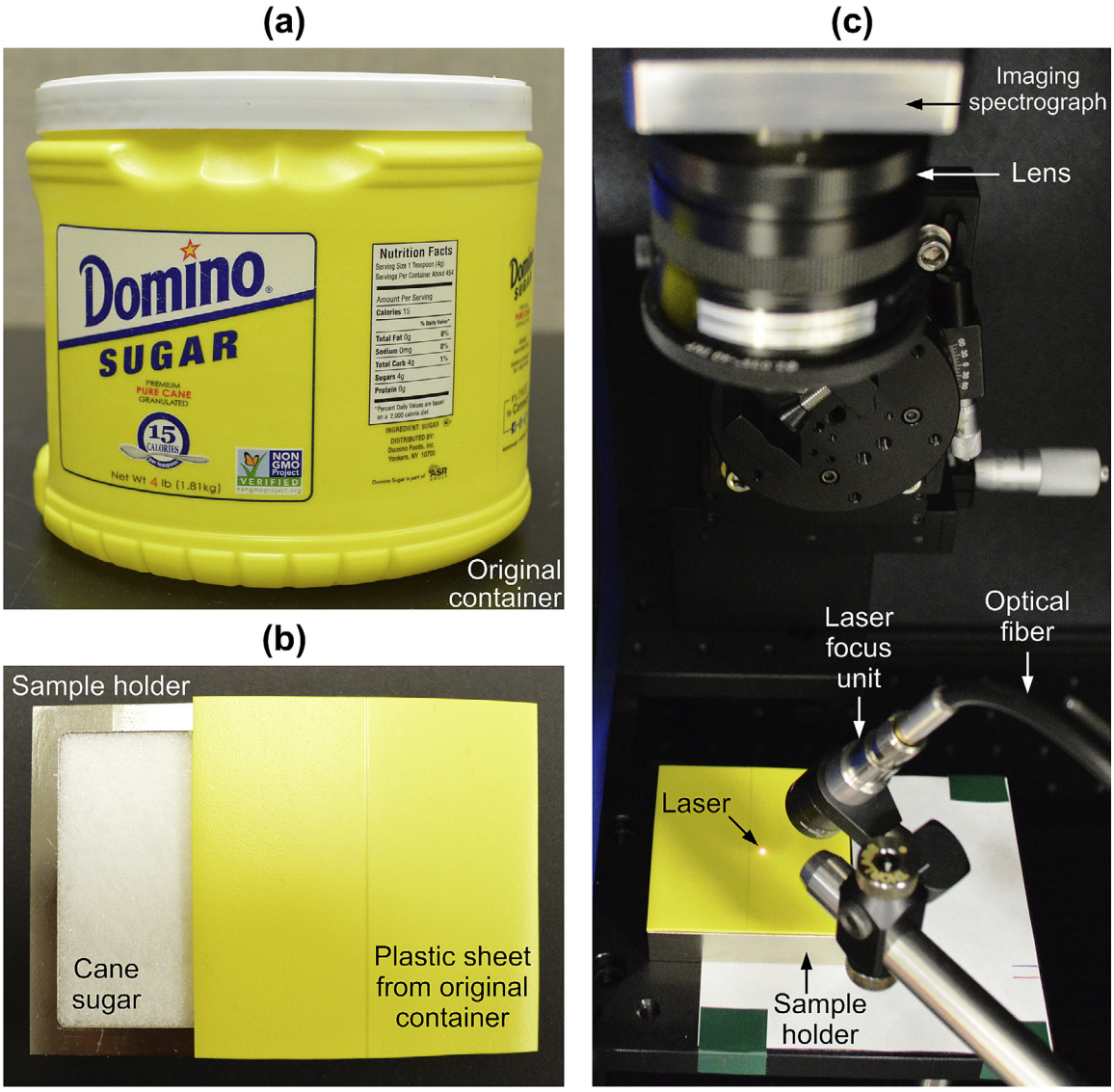

Fig. 3. Detection of sugar through plastic packaging: (a) cane sugar in original container, (b) plastic sheet from original container on top of a sample holder for sugar sample, and (c) line-scan spatially offset Raman spectroscopy measurement.

Fig. 4a shows Raman scattering images of the plastic sheet and the cane sugar as well as the plastic-on-sugar sample in a wavenumber range of 0–2815 cm^{-1} and a spatial range of 20 mm (including two identical offset ranges of 0–10 mm on the left and right sides of the incident laser). The scattering patterns in the images revealed both spatial and spectral features for the SORS measurements. A long scattering distance along the spatial dimension is generally corresponding to a Raman peak in the spectral dimension, whereas a narrowing of the bright area is usually the result of weak scattering signals. The longest scattering distances for plastic and sugar occurred at 1438 and 531 cm^{-1} (marked as two horizontal lines in Fig. 4a), which are corresponding to the Raman shift positions for the highest peaks of plastic and sugar, respectively. The scattering pattern of the plastic-on-sugar sample exhibited similarities with those of the plastic and the sugar owing to the Raman scattering contributions from the two materials. The Raman signals of the cane sugar at the bottom layer (e.g., peak at 531 cm^{-1}) can be observed in the scattering image of the layered sample. Meanwhile, spatial profiles can be extracted along the horizontal axis at different wavenumbers, and they are peaked at the laser incident point (i.e., zero offset position) with the intensities declined symmetrically towards the left and right sides of the longer offset distances (Qin et al., 2016). After examining selected spatial profiles of the plastic-on-sugar sample (not shown), an offset range of 0–10 mm was chosen for the self-modeling mixture analysis since the data beyond 10 mm were too noisy to be useful. Also due to the symmetry of the spatial profiles, only the data on the right side of the incident laser was used in SMA.

On the other hand, each line parallel to the vertical spectral axis of the scattering image represents a Raman spectrum at a specific offset distance. Fig. 4c shows a set of spatially offset Raman spectra of the plastic-on-sugar sample. Six spectra were extracted from the Raman scattering image in an offset range of 0–10 mm with a spatial interval of 2 mm to demonstrate the general pattern of the SORS data. The original spectra were normalized at either 531 or 1438 cm^{-1} and also vertically shifted for the purpose of direct comparison. The Raman spectral information was mixed between the top layer of the plastic sheet and the bottom layer of the cane sugar. As the offset distances increased, the relative intensities of

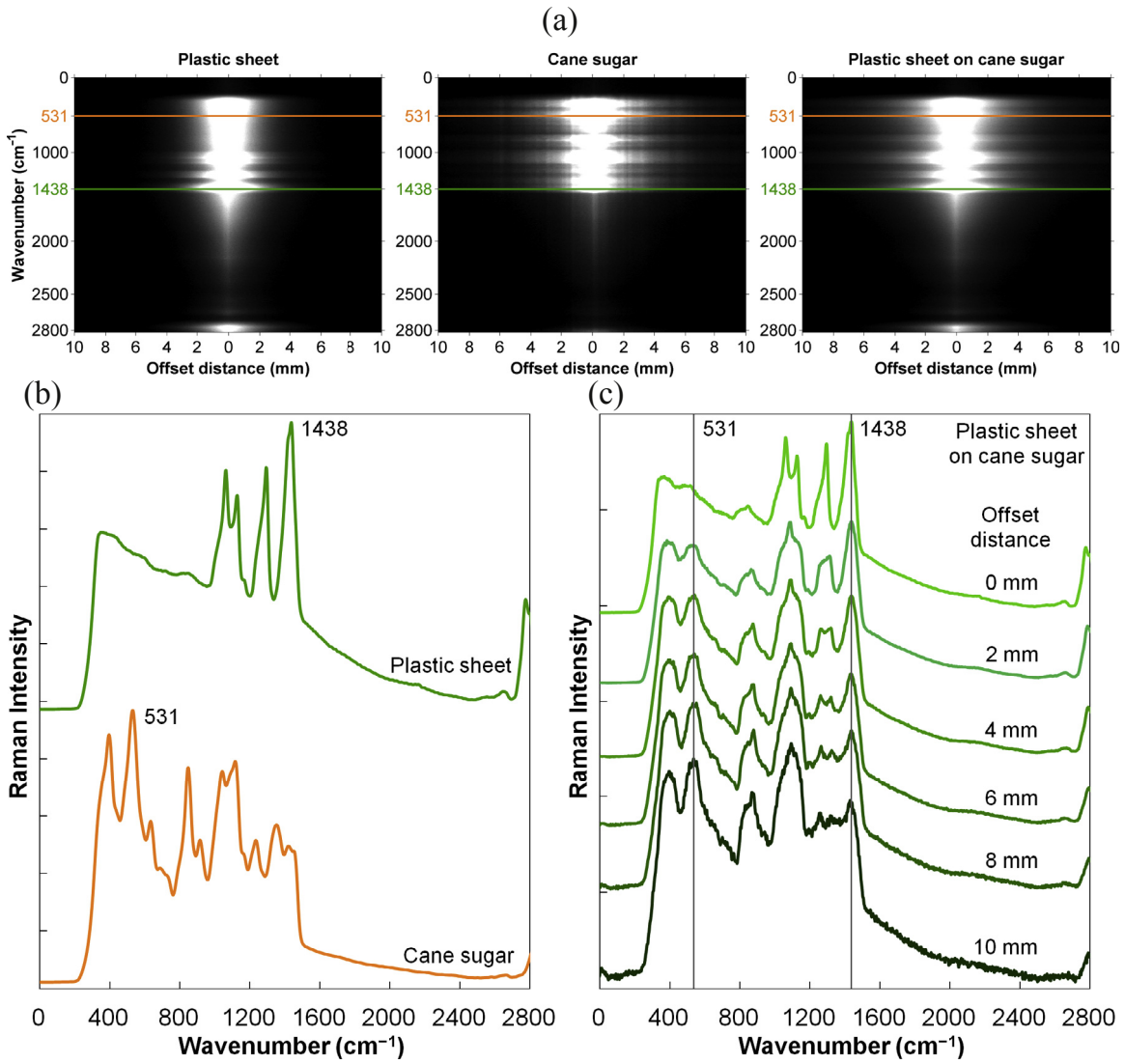

Fig. 4. (a) Raman scattering images of plastic sheet, cane sugar, and plastic-on-sugar sample, (b) reference Raman spectra of plastic sheet and cane sugar, and (c) spatially offset Raman spectra of the plastic-on-sugar sample at selected offset distances.

the 1438 cm^{-1} peaks were gradually diminished, whereas those of the 531 cm^{-1} peaks were gradually augmented. At the 0 mm offset distance, which is equivalent to the conventional backscattering Raman measurement, the bottom layer of the cane sugar was almost not detectable as evidenced by a weak Raman peak around 531 cm^{-1}. However, the 531 cm^{-1} peaks were clearly observed in the SORS spectra beyond the offset distance of 2 mm, demonstrating the capability of the line-scan SORS technique for subsurface detection of the Raman-active analytes.

3.2. SORS measurement results for carrot and melamine samples

Fig. 5 shows the SORS measurement results for the carrot and melamine samples. Reference Raman spectra of carrot and melamine are shown in Fig. 5b. A small fluorescence shoulder appeared in the low Raman shift region for the spectrum of the carrot, whereas the melamine showed a flat baseline without notable fluorescence signals. Three Raman peaks are shown in the carrot spectrum in the wavenumber range from 900 to 1600 cm^{-1}. The main Raman features of the melamine are in the wavenumber range of 300–1600 cm^{-1}. The highest Raman peaks of carrot and melamine were observed at 1513 and 673 cm^{-1}, respectively. The 1513 cm^{-1} and the 673 cm^{-1} vibrational modes are assignable respectively to carotenoids in carrot (Schulz, Baranska, & Baranski, 2005) and to NH_2 in-plane bending in the planar polynuclear aromatic structure of melamine ($(((-C-NH_2)=N-)_3$) (Schmidt et al., 2015). Since melamine does not have a Raman peak at 1513 cm^{-1} and carrot does not have a Raman peak at 673 cm^{-1}, the 1513 cm^{-1} peak of the carrot and the 673 cm^{-1} peak of the melamine were selected to identify and differentiate the two materials in the scattering images and the spatially offset Raman spectra.

The 2-D spatial-spectral images of the carrot and the melamine as well as the carrot-on-melamine sample are shown in Fig. 5a. Two horizontal lines were marked at 1513 and 673 cm^{-1} in each image to indicate the presence of the carrot and the melamine, respectively. Similar to the findings from Fig. 4a, the longest scattering distances for the carrot and the melamine appeared at 1513 and 673 cm^{-1}, respectively. The scattering patterns of the carrot and the melamine were clearly different owing to their different Raman characteristics. The scattering image of the carrot-on-melamine appeared similar to that of the carrot at the surface layer, while the Raman signals of the melamine at the subsurface layer (e.g.,

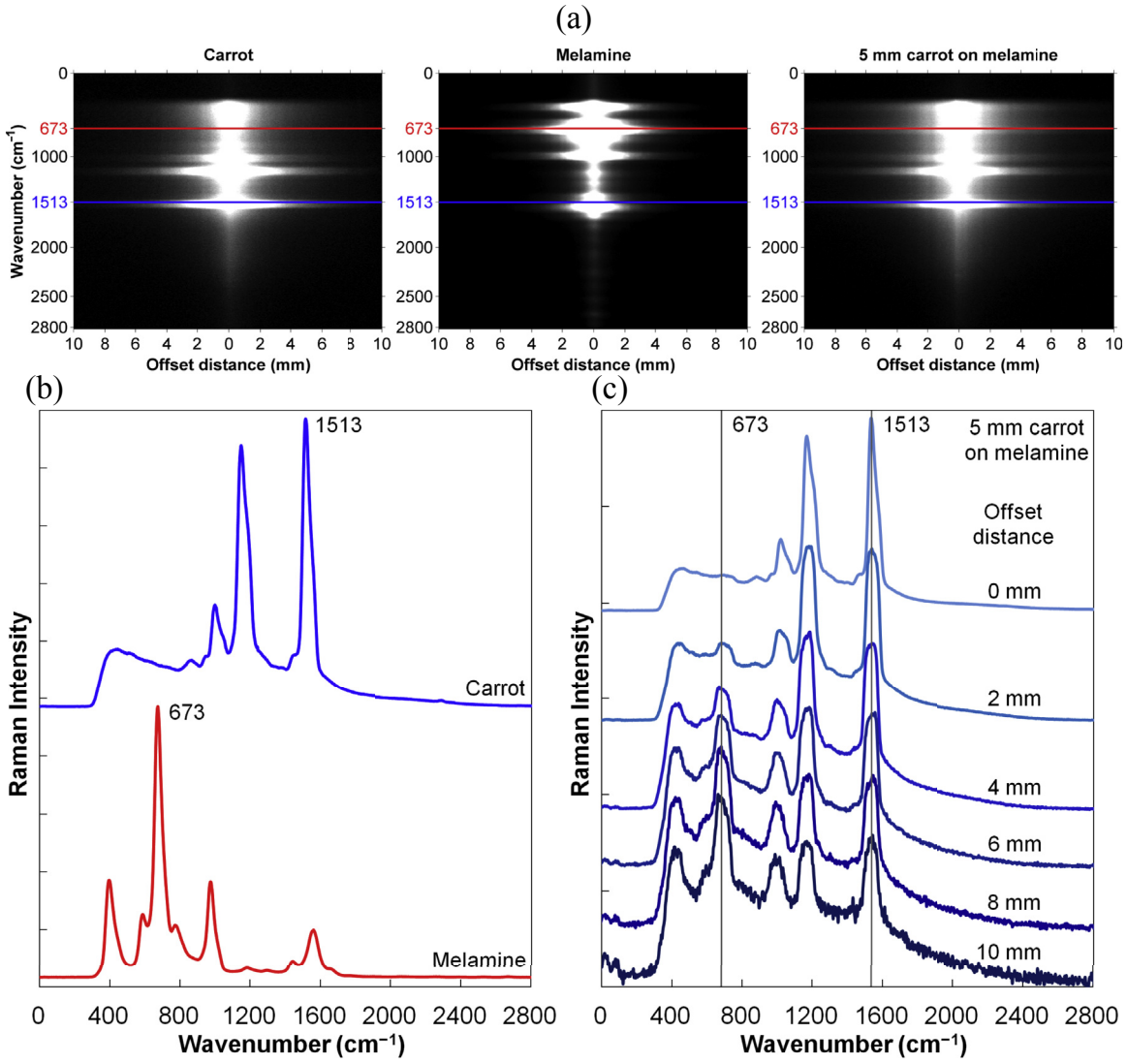

Fig. 5. (a) Raman scattering images of carrot, melamine, and carrot-on-melamine sample, (b) reference Raman spectra of carrot and melamine, and (c) spatially offset Raman spectra of the carrot-on-melamine sample at selected offset distances.

peak at 673 cm^{-1}) were observed through the 5 mm thick carrot slice. The spatial profiles extracted from the carrot-on-melamine sample image were also examined, and the SORS data on the right side of the incident laser in the offset range of 0–10 mm was used for SMA.

A set of spatially offset Raman spectra acquired from the layered carrot-on-melamine sample are shown in Fig. 5c. Similar to the plastic-on-sugar sample, six spectra were extracted from the Raman scattering image in an offset range of 0–10 mm with a spatial interval of 2 mm. The original spectra were normalized at either 673 or 1513 cm^{-1} and also vertically shifted for the purpose of direct comparison. The Raman information from the top layer of the carrot and the bottom layer of the melamine was mixed in the spatially offset spectra. With the increasing offset distances, the relative Raman intensities at 1513 cm^{-1} were gradually attenuated, whereas those at 673 cm^{-1} were gradually enhanced. The subsurface layer of the melamine was not detected from the spectrum at the 0 mm offset distance since no Raman peak was observed at 673 cm^{-1}. However, the 673 cm^{-1} peaks were shown in the SORS spectra beyond the offset distance of 2 mm. These results along with those from the plastic-on-sugar sample suggested that the line-scan SORS technique can detect the subsurface Raman signals, which usually exceeds the capability of the conventional backscattering Raman spectroscopy technique.

3.3. Self-modeling mixture analyses for subsurface detection of layered samples

The pure component spectra obtained from self-modeling mixture analyses for the plastic-on-sugar sample and the carrot-on-melamine sample are shown in Figs. 6 and 7, respectively. For each sample, the resolved spectra were identified based on visual examination of their similarities with the reference Raman spectra, and then were plotted in two groups with the corresponding reference spectra. The identification process can also be automatically executed for more complicated mixtures using spectral similarity metrics, such as spectral angle mapper (SAM) and spectral information divergence (SID) (Qin, Chao, & Kim, 2013). For the two layered samples, the two pairs of the resolved spectra shown in Figs. 6 and 7 were both the first two spectra from SMA using four components. No obvious Raman features were identified from the other two resolved spectra for each sample (not shown), and they

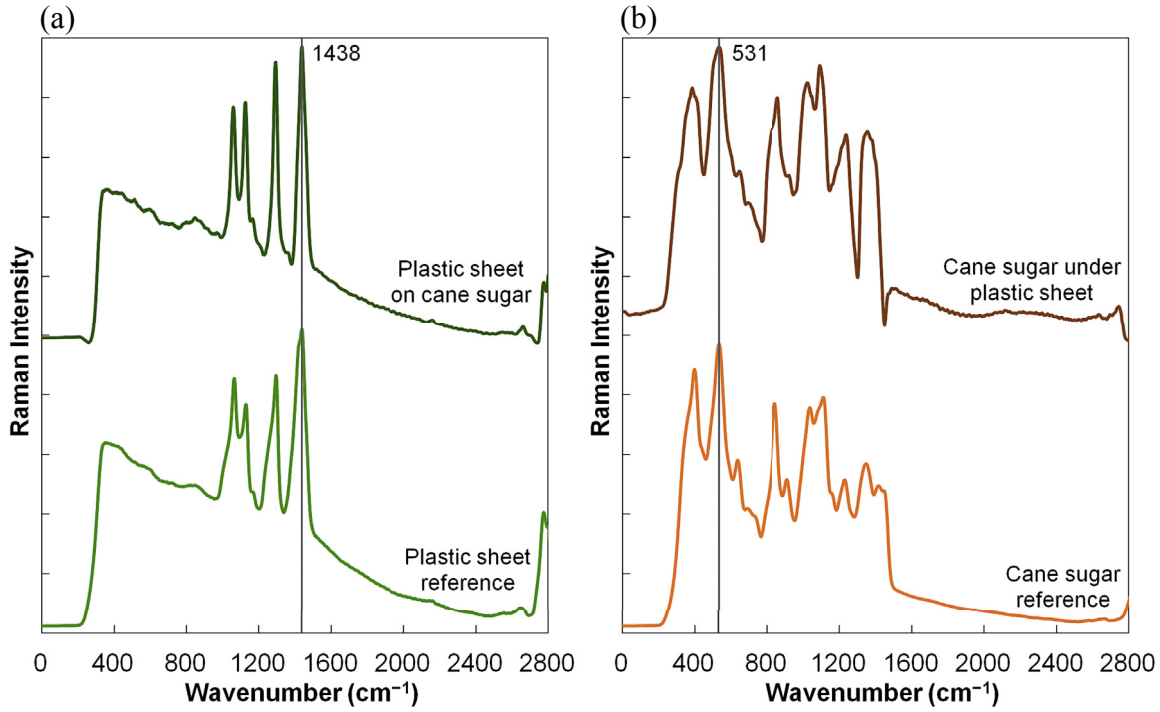

Fig. 6. Pure component spectra from self-modeling mixture analysis for the layered plastic-on-sugar sample: (a) plastic sheet on cane sugar and (b) cane sugar under plastic sheet.

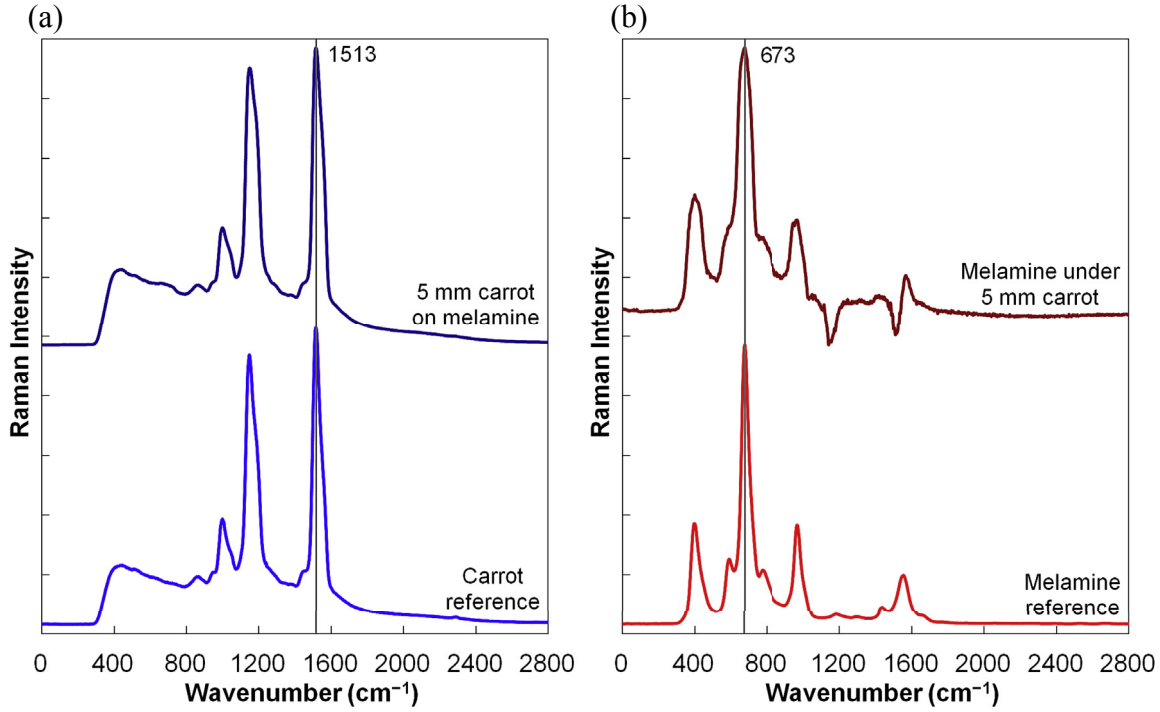

Fig. 7. Pure component spectra from self-modeling mixture analysis for the layered carrot-on-melamine sample: (a) 5 mm carrot on melamine and (b) melamine under 5 mm carrot.

likely represented the residual noises generated from the matrix decompositions in SMA.

As shown in Figs. 6 and 7, the Raman spectra from the top layers (i.e., plastic sheet and carrot) and the bottom layers (i.e., cane sugar and melamine) were successfully separated using SMA for the two layered samples. The pure component spectra plotted in Figs. 6a and 7a recovered all the major Raman features (e.g., peak positions and relative intensities) of the plastic sheet and the carrot, respectively. Also, the main Raman peaks of the cane sugar under the plastic sheet and the melamine under the carrot were retrieved in the resolved spectra (Figs. 6b and 7b), demonstrating the effectiveness of the line-scan SORS technique and SMA for

detecting the individual chemical information from the layered samples. In the resolved spectra, the Raman peaks of the cane sugar and the melamine at the bottom layers were not as sharp as those from their corresponding reference spectra. The reason can likely be attributed to the interferences of the top layers with the laser (from top to bottom) and with the Raman scattering signals from the bottom layers (from bottom to top). Regardless of the spectral shapes, the Raman peaks detected at 531 cm^{-1} for the cane sugar and at 673 cm^{-1} for the melamine as well as peaks at other wavenumbers indicated that the 785 nm point laser can penetrate the 1 mm thick plastic sheet and the 5 mm thick carrot slice in the SORS measurements and obtain the Raman signals from the underneath Raman-active analytes using the SMA method. The two example applications presented above demonstrated that the line-scan SORS technique can be used for rapid and nondestructive subsurface inspection of food safety and quality, such as authentication of foods and ingredients through packaging, evaluation of internal quality and/or maturity of fruits and vegetables, and detection of contaminants in deep areas of food and agricultural products.

4. Conclusions

This research has presented a method for subsurface inspection of food and agricultural products using a newly developed line-scan spatially offset Raman spectroscopy technique. The line-scan SORS technique is more flexible and efficient than the optical fiber probe approach in that it is able to collect a series of Raman spectra all together in a broad offset range with a narrow spatial interval using one CCD exposure. The scattering image acquired from a single scan is a complete set of spatially offset Raman spectra with sufficient spatial and spectral information for subsurface evaluation of heterogeneous or layered food samples. The Raman scattering signals from the cane sugar under the plastic sheet and the melamine powder under the carrot slice were successfully detected using the line-scan SORS system and the self-modeling mixture analysis algorithms. The two example applications demonstrated the capability of the line-scan SORS technique for authenticating foods and ingredients through packaging and evaluating internal food safety and quality attributes. The line-scan SORS measurement technique has great potential to be used for rapid and nondestructive subsurface inspection of food safety and quality.

References

Afseth, N. K., Bloomfield, M., Wold, J. P., & Matousek, P. (2014). A novel approach for subsurface through-skin analysis of salmon using spatially offset Raman spectroscopy (SORS). *Applied Spectroscopy, 68*(2), 255–262.

Arruebarrena de Báez, M., Hendra, P. J., & Judkins, M. (1995). The Raman spectra of oriented isotactic polypropylene. *Spectrochimica Acta Part A: Molecular and Biomolecular Spectroscopy, 51*, 2117–2124.

Awad, T. S., Moharram, H. A., Shaltout, O. E., Asker, D., & Youssef, M. M. (2012). Applications of ultrasound in analysis, processing and quality control of food: A review. *Food Research International, 48*, 410–427.

Brizuela, A. B., Bichara, L. C., Romano, E., Yurquina, A., Locatelli, S., & Brandán, S. A. (2012). A complete characterization of the vibrational spectra of sucrose. *Carbohydrate Research, 361*, 212–218.

Dam, J. S., Pedersen, C. B., Dalgaard, T., Fabricius, P. E., Aruna, P., & Andersson-Engels, S. (2001). Fiber-optic probe for noninvasive real-time determination of tissue optical properties at multiple wavelengths. *Applied Optics, 40*(7), 1155–1164.

Eliasson, C., & Matousek, P. (2007). Noninvasive authentication of pharmaceutical products through packaging using spatially offset Raman spectroscopy. *Analytical Chemistry, 79*(4), 1696–1701.

Hwang, J., Kang, S., Lee, K., & Chung, H. (2012). Enhanced Raman spectroscopic discrimination of the geographical origins of rice samples via transmission spectral collection through packed grains. *Talanta, 101*, 488–494.

Hyde, D. E., Farrell, T. J., Patterson, M. S., & Wilson, B. C. (2001). A diffusion theory model of spatially resolved fluorescence from depth-dependent fluorophore concentrations. *Physics in Medicine and Biology, 46*(2), 369–383.

Keller, M. D., Vargis, E., Granja, N., Wilson, R. H., Mycek, M., Kelley, M. C., et al. (2011). Development of a spatially offset Raman spectroscopy probe for breast tumor surgical margin evaluation. *Journal of Biomedical Optics, 16*(7), 077006.

Mathanker, S. K., Weckler, P. R., & Bowser, T. J. (2013). X-ray applications in food and agriculture: A review. *Transactions of the ASABE, 56*(3), 1227–1239.

Matousek, P., Clark, I. P., Draper, E. R. C., Morris, M. D., Goodship, A. E., Everall, N., et al. (2005). Subsurface probing in diffusely scattering media using spatially offset Raman spectroscopy. *Applied Spectroscopy, 59*, 393–400.

Matousek, P., Draper, E. R. C., Goodship, A. E., Clark, I. P., Ronayne, K. L., & Parker, A. W. (2006). Noninvasive Raman spectroscopy of human tissue in vivo. *Applied Spectroscopy, 60*, 758–763.

Matousek, P., & Parker, A. W. (2006). Bulk Raman analysis of pharmaceutical tablets. *Applied Spectroscopy, 60*(12), 1353–1357.

Qin, J., Chao, K., Cho, B., Peng, Y., & Kim, M. S. (2014). High-throughput Raman chemical imaging for rapid evaluation of food safety and quality. *Transactions of the ASABE, 57*(6), 1783–1792.

Qin, J., Chao, K., & Kim, M. S. (2012). Nondestructive evaluation of internal maturity of tomatoes using spatially offset Raman spectroscopy. *Postharvest Biology and Technology, 71*, 21–31.

Qin, J., Chao, K., & Kim, M. S. (2013). Simultaneous detection of multiple adulterants in dry milk using macro-scale Raman chemical imaging. *Food Chemistry, 138*(2–3), 998–1007.

Qin, J., Kim, M. S., Schmidt, W. F., Cho, B., Peng, Y., & Chao, K. (2016). A line-scan hyperspectral Raman system for spatially offset Raman spectroscopy. *Journal of Raman Spectroscopy, 47*(4), 437–443.

Qin, J., & Lu, R. (2008). Measurement of the optical properties of fruits and vegetables using spatially resolved hyperspectral diffuse reflectance imaging technique. *Postharvest Biology and Technology, 49*(3), 355–365.

Schmidt, W. F., Broadhurst, C. L., Qin, J., Lee, H., Nguyen, J. K., Chao, K., et al. (2015). Continuous temperature-dependent Raman spectroscopy of melamine and structural analog detection in milk powder. *Applied Spectroscopy, 69*(3), 398–406.

Schmidt, S. J., Sun, X., & Litchfield, J. B. (1996). Applications of magnetic resonance imaging in food science. *Critical Reviews in Food Science and Nutrition, 36*(4), 357–385.

Schulmerich, M. V., Walsh, M. J., Gelber, M. K., Kong, R., Kole, M. R., Harrison, S. K., et al. (2012). Protein and oil composition predictions of single soybeans by transmission Raman spectroscopy. *Journal of Agricultural and Food Chemistry, 60*(33), 8097–8102.

Schulz, H., Baranska, M., & Baranski, R. (2005). Potential of NIR–FT–Raman spectroscopy in natural carotenoid analysis. *Biopolymers, 77*, 212–221.

Shin, K., Chung, H., & Kwak, C. W. (2012). Transmission Raman measurement directly through packed corn kernels to improve sample representation and accuracy of compositional analysis. *Analyst, 137*(16), 3690–3696.

Wang, Z., Ding, H., Lu, G., & Bi, X. (2014). Use of a mechanical iris-based fiber optic probe for spatially offset Raman spectroscopy. *Optics Letters, 39*(13), 3790–3793.

Windig, W., & Guilment, J. (1991). Interactive self-modeling mixture analysis. *Analytical Chemistry, 63*(14), 1425–1432.

Xiong, C., Li, G., & Lin, L. (2012). Composition analysis of scattering liquids based on spatially offset visible-near-infrared spectroscopy. *Applied Spectroscopy, 66*(11), 1347–1352.